

A First-in-Human Phase I Study of Subcutaneous Outpatient Recombinant Human IL15 (rhIL15) in Adults with Advanced Solid Tumors



Jeffrey S. Miller¹, Chihiro Morishima², Douglas G. McNeel³, Manish R. Patel¹, Holbrook E.K. Kohrt⁴, John A. Thompson^{5,6}, Paul M. Sondel³, Heather A. Wakelee⁴, Mary L. Disis², Judith C. Kaiser², Martin A. Cheever², Howard Streicher^{5,6}, Steven P. Creekmore^{5,6}, Thomas A. Waldmann^{5,6}, and Kevin C. Conlon^{5,6}

Abstract

Purpose: Preclinical data established IL15 as a homeostatic factor and powerful stimulator of NK and CD8⁺ T-cell function, the basis for clinical testing.

Experimental Design: A first-in-human outpatient phase I dose escalation trial of subcutaneous (SC) rhIL15 was conducted in refractory solid tumor cancer patients. Therapy consisted of daily (Monday–Friday) subcutaneous injections of rhIL15 for two consecutive weeks (10 total doses/cycle). Clinical response was assessed by RECIST. Pharmacokinetics of rhIL15 and immune biomarkers were evaluated.

Results: Nineteen patients were treated with rhIL15 at dose levels of 0.25, 0.5, 1, 2, and 3 mcg/kg/day. Fourteen patients completed ≥ 2 cycles of therapy that was well tolerated. One serious adverse event (SAE), grade 2 pancreatitis, required overnight hospitalization. Enrollment was halted after a patient

receiving 3 mcg/kg/day developed a dose-limiting SAE of grade 3 cardiac chest pain associated with hypotension and increased troponin. No objective responses were observed; however, several patients had disease stabilization including a renal cell carcinoma patient who continued protocol treatment for 2 years. The treatment induced profound expansion of circulating NK cells, especially among the CD56^{bright} subset. A proportional but less dramatic increase was found among circulating CD8⁺ T cells with maximal 3-fold expansion for the 2 and 3 mcg/kg patients.

Conclusions: SC rhIL15 treatment was well tolerated, producing substantial increases in circulating NK and CD8⁺ T cells. This protocol establishes a safe outpatient SC rhIL15 regimen of 2 mcg/kg/day dosing amenable to self-injection and with potential as a combination immunotherapeutic agent. *Clin Cancer Res*; 24(7); 1525–35. ©2017 AACR.

Introduction

Positive reports from clinical trials evaluating immune checkpoint inhibitors, antitumor mAbs and adoptive cellular therapies have refocused oncologic drug development on immune-based investigational agents (1–7). While immune checkpoint inhibitors have appreciable activity in several solid tumor types not typically considered immunosensitive (8–10) and whereas cellular therapies using cells with genetically manipulated chimeric antigen receptor cells (CAR) have impressive activity in several leukemias, these therapies have ultimately been demonstrated to be effective in only a minority of advanced cancer patients seeking

therapy (7, 11–14). Natural killer (NK) cell therapy is also promising in acute myeloid leukemia with 30%–50% remission reported after NK-cell infusions (15, 16). Our evolving understanding of a productive antitumor immune response hypothesizes that infiltration of tumors by activated tumor antigen (Ag)-specific lymphocytes capable of sustained activity is critical for clinical activity (17, 18). Continued support or stimulation of these effector cells requires sustained production of stimulatory cytokines and mitigation of the immunosuppressive effects of CD4⁺ CD25⁺ FoxP3⁺ T regulatory (Treg) cells and myeloid-derived suppressor cells (MDSC; refs. 19–22).

IL15 is a homeostatic factor for NK and T cells and is required for NK-cell development. Like IL2, IL15 potentiates NK-cell antitumor activity *in vitro* and *in vivo* (23–30). Experiments demonstrated that IL15 improved the survival of mice in established models of MC38 and CT-25 colorectal carcinomas (31, 32). In the transgenic murine melanoma Pmel model, IL15 was shown to stimulate a potentially curative antigen-specific CD8⁺ T-cell response that was also synergistic with other common gamma chain cytokines (33). Coadministration of IL15 with the fowlpox TRICOM and gp160 vaccines further demonstrated synergistic activity producing long-lasting antigen-specific CD8⁺ T-cell responses against renal cell carcinoma and HIV, respectively, that was superior to these vaccines plus IL2 (34). These experiments, among others, have established IL15 as an immunotherapeutic that activates NK cells and CD8⁺ T cells, sustains long-term

¹University of Minnesota, Minneapolis, Minnesota. ²University of Washington, Seattle, Washington. ³University of Wisconsin, Madison, Wisconsin. ⁴Stanford University, Palo Alto, California. ⁵Fred Hutchinson Cancer Research Center, Seattle, Washington. ⁶National Cancer Institute/NIH, Bethesda, Maryland.

Note: J.S. Miller and C. Morishima are the co-first authors of this article.

T.A. Waldmann and K.C. Conlon are the co-senior authors of this article.

Corresponding Author: Jeffrey S. Miller, Division of Hematology, Oncology, and Transplantation, University of Minnesota, 420 Delaware St. SE, Mayo Mail Code 806, Minneapolis, MN 55455. Phone: 612-625-7409; Fax: 612-626-3941; E-mail: mille011@umn.edu

doi: 10.1158/1078-0432.CCR-17-2451

©2017 American Association for Cancer Research.

Translational Relevance

Preclinical experiments demonstrated that IL15 can control homeostasis and stimulate natural killer (NK) and antigen-specific CD8⁺ T-cell activity without causing activation-induced cell death (AICD) or promoting T regulatory (Treg) cell function. Recognition of these properties led to the designation of IL15 as the immunotherapeutic with highest potential for clinical development by the 2007 NCI Immunotherapy Workshop. Unexpected toxicities encountered in the first-in-human clinical trial of recombinant human (rh) IL15 given as daily 30-minute intravenous bolus (IVB) infusions severely limited dose escalation. Preclinical and nonhuman primate toxicology experiments suggested that subcutaneous administration should lower peak concentrations and improve clinical tolerance. This is a first-in-human experience with outpatient subcutaneous rhIL15, allowing 6-fold more drug delivery than IVB, and inducing robust levels of immune activation. These results will allow the export of IL15 immunotherapy to an outpatient setting and testing of combinatorial strategies to improve cancer treatment.

memory T cells, inhibits activation-induced cell death (AICD), and does not promote the activity of regulatory T cells (Treg; refs. 26–29). The biologic effects of IL15 compare very favorably with IL2, the prototypic immunotherapeutic cytokine that is occasionally administered to metastatic melanoma and renal cell carcinoma patients. Despite durable and sometimes complete responses, the small percentage of responders and significant clinical toxicities of high-dose intravenous bolus IL2 (HDIL2) treatment limit its use (35, 36). In the first-in-human phase I clinical trial of recombinant human (rh)IL15, treatment was given as a 30-minute infusion (IVB) once daily for 12 consecutive days (37). Dose escalation was constrained by postinfusion toxicities of fevers, rigors, and transiently decreased blood pressure, although less problematic than similar HDIL2 toxicities. Moreover, rhIL15 IVB resulted in lower MTD (0.3 mcg/kg IVB) and immune activation than was anticipated on the basis of the nonhuman primate toxicology experiments. Coincidental to this first-in-human rhIL15 clinical trial, additional nonhuman primate experiments demonstrated that sustained administration regimens of rhIL15 by either continuous intravenous infusion (CIV) or subcutaneous injection produced substantially greater immune activation with less toxicity and possibly greater clinical potential than the initial IVB regimen (30). On the basis of these preclinical data and the clinical experience in the first-in-human rhIL15 IVB trial, this phase I dose escalation trial of SC rhIL15 administered by daily injection Monday through Friday for 2 consecutive weeks of a 28-day cycle was initiated. The goal of this study was to design a safe outpatient regimen that could be used alone or in combinatorial strategies. The safety, pharmacokinetics, correlative immunologic laboratory analyses, and clinical activity of this treatment regimen are reported.

Materials and Methods

Patients

Patients with advanced metastatic melanoma, renal cell carcinoma (RCC), non-small cell lung (NSCLC), and squamous cell

head and neck carcinoma (SCCHN) were enrolled in this phase I open-label, nonrandomized dose escalation study. Eligible patients were required to be age \geq 18 years, have histologically confirmed metastatic solid tumors, failed at least 1 prior standard treatment regimen, have ECOG performance status 0 or 1, absolute lymphocyte count (ALC) $>500/\text{mL}$, absolute neutrophil count (ANC) $>1,000/\text{mL}$, platelets $>100,000/\text{mL}$, total bilirubin within normal institutional limits, PT/PTT $<1.5\times$ institutional upper limit of normal (ULN), nontransfused hemoglobin $>9\text{ g/dL}$, alkaline phosphatase $\leq 2.5\times$ ULN, AST/ALT <2 ULN, serum creatinine $<1.5\times$ ULN, absence of CNS metastases, no history of clinically significant autoimmune disease or hematopoietic malignancy, no history of severe asthma, no use of systemic corticosteroid treatment or inhaled steroids, no evidence of clinically active infection, no history of or serology positive for HIV or hepatitis B or C or HTLV-1, and no clinically significant congestive (NYHA class II or greater) heart disease. Pregnant female patients were excluded, and patients must have been more than 4 weeks from their most recent treatment, 6 weeks for nitrosoureas/mitomycin, 8 weeks for anti-CTLA4 or anti-PD1, more than 2 weeks from radiotherapy, have recovered from previous treatment, not receiving any other investigational treatment and able to give informed consent.

Study design

This trial was sponsored and overseen by the Cancer Immunotherapy Trials Network (CITN) and conducted at 5 clinical centers in the United States [University of Wisconsin (Madison, WI), University of Minnesota (Minneapolis, MN), Stanford University (Stanford, CA), Seattle Cancer Care Alliance (Seattle, WA), and the National Cancer Institute/NIH (NCI/NIH, Bethesda, MD)] between July 2013 and March 2016. This protocol was approved and monitored by the Cancer Treatment Evaluation Program (CTEP)/NCI/NIH. The Fred Hutchinson Cancer Research Center Institutional Review Board (IRB) functioned as the Central IRB for this study and for three of the respective enrolling institutions. The primary objective was to define the MTD for this subcutaneous rhIL15 regimen. A standard 3 + 3 phase I design was employed that enrolled at least 3 patients at each dose level, with dose escalation proceeding in the absence of dose-limiting toxicity (DLT) occurring during the first treatment cycle. If a DLT occurred in one of the first 3 patients enrolled at a dose level, the cohort size was expanded to 6 patients. If ≥ 2 of 3 or 6 patients experienced DLTs, dose escalation would be halted and the prior level considered the MTD. The NCI Common Toxicity Criteria version 4 (CTCv4) was used to assess adverse events (AE) with DLTs being defined as any \geq grade 3 toxicity with nonhematologic exceptions based on previous clinical studies with rhIL15 that included grade 3 fatigue or anorexia, grade 3 hypocalcemia, hypokalemia, hypomagnesemia, hyponatremia, hypophosphatemia that responded to medical intervention, temperature $> 40^\circ\text{C}$ for <48 hours, febrile neutropenia not requiring urgent intervention; hematologic exceptions were grade 3 or 4 lymphopenia, grade 3 neutropenia, and grade 3 lymphocyte increase. $\text{ALC} > 25,000/\text{mm}^3$ was also not considered a DLT, but was designated the "maximum desired effect" and would prompt interruption of treatment until the lymphocyte count dropped without precluding additional subsequent treatment. However, $\text{ALC} > 35,000/\text{mm}^3$ was considered a DLT.

Study treatment

The investigational agent used in this trial was *E. coli*-derived rhIL15 manufactured by the Biopharmaceutical Development Program (BDP) of the Division of Cancer Treatment and Diagnosis (DCTD)/NCI using current Good Manufacturing Practices (cGMP). Study drug was provided to the treating centers by the Pharmaceutical Management Branch/DCTD. Treatment cycles were 28 days in length with patients receiving daily SC rhIL15 on days 1 through 5 and 8 through 12 at dose levels of 0.25, 0.5, 1, 2, and 3 mcg/kg/day. Injection sites were rotated to different areas of the body (upper and lower extremities, each of the 4 quadrants of the abdomen) to minimize the summated local effects of drug administration. Routine premedication with antipyretics or nonsteroidal anti-inflammatory agents such as acetaminophen, ibuprofen, naproxen, or aspirin at established doses and schedules were given at the treating physician's discretion. Additional concomitant antiemetics, anti-diarrheals, intravenous fluids or electrolyte replacement based on clinical or laboratory assessments and blood transfusions while on treatment based on individual institutional guidelines were allowed.

Clinical and investigational assessments

Standard clinical assessment of the patients included routine monitoring of vital signs, appraisal of adverse events (AE), injection site reactions, routine chemistry panels, and complete blood count (CBC) on each treatment day. A detailed history and physical (H&P) exam was performed on day 1 and day 8 and focused H&P on all other treatment days. Serum samples to detect anti-IL15 antibodies were collected prior to day 1 dosing of each cycle of treatment, and 6 months after treatment was completed from a select group of patients. Limited rhIL15 pharmacokinetic analysis was performed during cycle 1 with serum samples obtained immediately prior to the first dose of study drug (baseline), then at 10 minutes, 1, 4, and 24 hours after the initial treatment to assess serum IL15 levels, as well as inflammatory cytokines. Heparinized whole-blood samples were also obtained at baseline, day 11, and day 15 (72 hours after completion of treatment) during each cycle for immunophenotyping of peripheral blood mononuclear cells (PBMC), and NK cellular function assessment at cycle 1 time points.

Specimen handling and processing

Heparinized whole-blood samples collected at each clinical site were shipped by overnight express mail in insulated shippers that contained LogTag temperature recorders to continuously record ambient temperatures during shipment. Samples were received at the University of Washington CITN Central Laboratory an average of 28 hours later. Aliquots of fresh whole blood were immediately used for real-time antibody labeling for flow cytometric analyses and the remainder of the samples processed to plasma and PBMCs using standard Ficoll-Hypaque isolation immediately upon receipt. PBMCs were cryopreserved in 10% DMSO (Sigma) and 12.5% HSA (Gemini) at -80°C and subsequently maintained in vapor phase liquid nitrogen freezers. Cryopreserved PBMC samples were shipped to the University of Minnesota for functional lymphocyte testing in Cryoport liquid nitrogen shippers. Serum was collected at the clinical sites within 4 hours of blood draw and frozen at -80°C . Batched samples were later shipped on dry ice to the CITN Central Laboratory and then subsequently to the NCI for testing (38).

Correlative flow cytometry and cellular cytotoxicity analyses

Immunophenotyping. Whole-blood flow cytometric analyses were performed initially using day 1 and 11 time point samples. The protocol was amended in April 2014 to add flow cytometric testing on day 15 of each cycle to better assess the posttreatment lymphocytosis suggested by other studies to be maximal 3 days after completion of the rhIL15 injections. Fresh whole-blood samples were labeled with fluorescently labeled antibodies to cell surface molecules CD45 (2D1), CD3 (UCHT1), CD8 (SK1), CD56 (NCAM16.1), CD16 (3G8), CD14 (MOP9), CD123 (9FS; all BD Biosciences) and CD4 (RPA-T4), CD19 (HIB19), and HLA-DR (L243; all Biolegend) after overnight shipping to the CITN Central Lab, using a method adapted from Hensley and colleagues (38). Samples were treated with BD FACS Lysing Solution (BD Biosciences) and immediately frozen at -80°C for later batch testing on a BD LSRII flow cytometer. Absolute cell numbers were obtained using Trucount tubes (BD Biosciences). Data analysis was performed using FlowJo software (Treestar).

Functional lymphocyte evaluation. Cryopreserved PBMCs were thawed, washed once in PBS + 0.3% BSA, then resuspended in RPMI1640 with 10% FCS without cytokines at a cellular concentration of $2 \times 10^6/\text{mL}$ and incubated at 37°C in 5% CO_2 until the functional assays were performed. After an 18- to 24-hour incubation, NK-cell activity was tested against K562 targets at an effector to target ratio of 2:1 in a 5-hour assay that assessed CD107a expression and intracellular TNF α production using the Transcription Factor Fixation/Permeabilization Concentrate and Diluent (eBioscience Thermo Fisher Scientific). The same buffer was used in the unstimulated Ki67 expression assay. Fluorescently labeled anti-human mAbs utilized were PE-Cy7-conjugated CD56 (HCD56), FITC or BV605-conjugated CD45 (H130), BV785-conjugated CD3 (OKT3), PerCP Cy5.5-conjugated CD107a (LAMP-1), BV421-conjugated TNF α (Mab11), and BV711-conjugated Ki67 (Ki67; all Biolegend). Cells were fixed with 2% paraformaldehyde and analyzed at one time on a BD LSRII flow cytometer. All results were analyzed using FlowJo software.

Pharmacokinetic analyses and detection of anti-rhIL15 antibodies.

PK and anti-rhIL15 antibody analyses of frozen serum samples were conducted at the Clinical Support Laboratory, Frederick National Laboratory for Clinical Research, (Leidos Biomedical Research, Frederick, MD). Serum rhIL15 concentrations were assessed using a human IL15-specific ELISA kit (R&D Systems) according to manufacturer's directions. Serum IL15 levels were analyzed using SoftMax Pro software version 5.2 or higher (37).

An ELISA developed by the Waldmann laboratory (NCI, Bethesda, MD) and previously used to monitor the development of anti-IL15 antibodies in NCI rhIL15 clinical trials (37) was used for this same purpose in baseline and pretreatment day 1 patient sera from all cycles. For this test, 100 ng/mL of rhIL15 was used to precoat 96-well microtiter plates, then plates washed and blocked with PBS/3% BSA. An affinity purified goat anti-human IL15 (R&D Systems) was used to define the standard curve. After overnight incubation with sera and controls at 4°C and washing, biotinylated IL15 was added for 2 hours at 37°C . Plates were washed, then streptavidin-alkaline phosphatase was added for 2 hours at 37°C . Plates were washed and then developed with p-nitrophenol phosphate for 1 hour at 37°C . Results were determined using

Miller et al.

SoftMax Pro Version 5.2 or higher. The lower limit of quantitation in undiluted serum is 156 ng/mL for this ELISA.

Evaluation of the neutralizing capacity of anti-IL15 antibodies. To detect antibodies that could specifically neutralize *E. coli* rhIL15 but not rhIL2 or endogenous heterodimeric IL15 (HetIL15), inhibition of IL15, or IL2-induced NK-92 proliferation by ³H-thymidine incorporation was measured (39). Briefly, serial dilutions of affinity-purified goat anti-human-IL15 were added to rhIL15-treated NK-92 cell cultures to produce a standard curve. To assess the neutralizing capability of anti-IL15 antibodies present in patient sera, serial dilutions of individual sera were added to rhIL15-treated NK-92 cell cultures and neutralizing antibody levels (ng/mL) calculated by comparison with the standard antibody curve.

Assay for serum inflammatory cytokines

The Meso Scale Discovery (MSD) V-PLEX immunoassay system was used to quantify serum concentrations of human IFN γ , IL1 β , IL6, IL10, IL12p70, and TNF α . Assays were performed according to manufacturer's instructions as described previously (37).

Statistical analysis

Characteristic statistics for a "3 + 3" phase I dose escalation trial where 2 of 3 patients in a dosing cohort [proportion 0.67 with 95% confidence intervals (CI), 21%–94%] or 2 of 6 patients in a dosing cohort (proportion 0.33 with 95% CI, 10%–70%) demonstrate that the MTD has been exceeded and the previous tolerable dose level represents the true MTD (40). For the laboratory studies, descriptive statistics were used as indicated.

Results

Patients and treatment

Twenty eligible patients were enrolled (one refused treatment after signing consent) and 19 patients were treated with SC rhIL15, including 9 with RCC, 6 with NSCLC, and 3 each with multiple myeloma or SCCHN (Table 1). The median age of the patients was 61 years (range 38–78) and approximately two-thirds were male. Patients enrolled into this trial were heavily pretreated and had

progressed or not responded following one or more systemic therapies. Six of 19 patients completed 4 treatment cycles; two of these patients received additional cycles as permitted by the study protocol and approved by CTEP. Most patients discontinued protocol therapy due to disease progression, but 3 patients stopped due to a treatment-related adverse event (AE), and 3 other patients completed the protocol therapy without significant toxicity or disease progression. Of those who stopped for an AE, one patient discontinued treatment when their pre-existing mild psoriasis became worse, a second patient discontinued treatment for an SAE of pancreatitis and the third patient for an SAE of DLT grade 3 cardiac chest pain. Approximately one-third of treated patients ($N = 7$) had disease stabilization and continued their outpatient treatment beyond 2 cycles, including a patient who remained on treatment for 2 years. The protocol was amended twice to increase the maximum number of treatment cycles when anti-IL15 antibodies were first identified in the absence of safety concerns, and second after it was determined that prolonged treatment of patients with disease stabilization may have resulted from study treatment. The decision to terminate the protocol before the MTD was formally defined was made by the study principal investigator in conjunction with the CITN Safety Committee after review of the AE profile for the 3 mcg/kg dose level, concluding that 2 mcg/kg most likely represented the MTD that could be administered safely as an outpatient regimen.

Dose escalation and treatment-related adverse events

Daily SC injections of rhIL15 were generally well tolerated, especially at the first 3 dose levels. The most common symptoms associated with treatment were as expected: fevers, chills, decreased blood pressure (BP), and injection site reactions (Table 2: AEs occurring in 5 or more subjects). Importantly, all injection site reactions that occurred at any dose level were grade 1 (2–4 mm of erythema) and no suggestion of recall events or increases in the severity of injection site reactions occurred during subsequent treatment cycles. Patients with decreased BP were all in the 2 or 3 mcg/kg dose cohorts except for 2 patients at the 0.5 mcg/kg dose level. Fatigue was noted in 9 of 19 patients, all grade 1, with the exception of 1 patient with grade 2 fatigue. Nausea and/or vomiting occurred in < half of patients, was mild, and was neither

Table 1. Subject demographics

Dose (mcg/kg)	Subject	Age	Gender	Cancer type	Cycles completed	Off-study for
0.25	1	75	M	Renal	2	Progression
0.25	2	61	M	Lung	4	Completed
0.25	3	55	M	Renal	4	Progression
0.5	4	38	F	Lung	4	Progression
0.5	5	74	M	Renal	24	Completed
0.5	6	58	F	Melanoma	2	Progression
1.0	7	71	M	SCCHN	1	Discontinued ^a
1.0	8	69	F	Lung	4	Completed
1.0	9	61	F	Melanoma	2	Progression
2.0	10	62	M	Melanoma	1	Adverse Event
2.0	11	59	M	Renal	2	Progression
2.0	12	77	M	Renal	2	Adverse event
2.0	13	60	M	Lung	6	Completed
2.0	14	44	M	SCCHN	2	Progression
2.0	15	53	M	Renal	2	Progression
3.0	16	78	F	Renal	4	Progression
3.0	17	75	M	SCCHN	1	Progression
3.0	18	59	F	Lung	1	Adverse Event
3.0	19	61	F	Lung	2	Progression

Abbreviation: completed, completed 4 cycles (or more) without disease progression; F, female; M, male.

^aResponse assessment not performed; patient discontinued study participation.

Table 2. Adverse events

Adverse event	# Subjects affected, total (%)	# Subjects affected, 2 and 3 mcg/kg (%)	Highest AE grade/dose cohort				
			0.25 mcg/kg	0.5 mcg/kg	1 mcg/kg	2 mcg/kg	3 mcg/kg
Injection site reaction	14 (74)	7 (70)	1	1	1	1	1
Chills	13 (68)	8 (80)	1	1	1	2	2
Anemia	12 (63)	7 (70)	2	2	2	2	2
Fever	11 (58)	10 (100)			1	2	3
Hypotension	10 (53)	8 (80)		1		2	2
Fatigue	9 (47)	6 (60)		1	1	1	2
Hypophosphatemia	9 (47)	5 (50)	3	3		3	2
Tachycardia	7 (37)	5 (50)	1	1		1	1
Vomiting	7 (37)	4 (40)	2	1	1	1	1
Hypoalbuminemia	7 (37)	4 (40)	3	2		1	2
Hypertension	7 (37)	3 (00)	2	3		3	1
Dry skin	6 (32)	5 (50)		1		1	2
Nausea	6 (32)	3 (30)	2		1	1	1
Lymphopenia	5 (26)	5 (50)				3	3
Elevated AST	5 (26)	4 (40)			1	1	2
Diarrhea	5 (26)	3 (30)	3	1		1	1

NOTE: Adverse events occurring in 5 more subjects is shown.

more common nor severe in the higher dose levels. The most common laboratory abnormalities were anemia, hypophosphatemia, thrombocytopenia and hypoalbuminemia, in that order of frequency. Some level of mild anemia was present in 12 of 19 patients. Seven of 19 patients experienced transient mild thrombocytopenia, defined as $<150,000/\text{mL}$, with a range of 112–134,000 (mean 125,000). Transient lymphopenia was reported only in the 2 and 3 mcg/kg dose cohorts, and mild neutropenia only occasionally occurred. Elevations in aspartate and/or alanine aminotransferase occurred in approximately 1 of 4 of patients treated in this protocol and were generally mild, but more common in the higher dose level cohorts.

One SAE of pancreatitis began approximately 2 days after the patient's last rhIL15 dose of cycle 1, requiring overnight hospitalization, pain medications, and acute alteration of his diet. Study treatment was discontinued and the patient recovered fully within a few weeks without sequelae. The third patient enrolled at the 3 mcg/kg dose level had grade 3 cardiac chest pain, an SAE and DLT. After supportive care and hospitalization for 1 day, this SAE resolved without sequelae. When two other patients treated at this dose level experienced grade 2 or 3 fevers, the decision was made to discontinue protocol treatment with the conclusion that 2 mcg/kg was likely the MTD for outpatient therapy.

Clinical response

The objective response rate was assessed according to RECIST 1.1 criteria guidelines by following marker lesions defined in baseline CT scans with radiographic restaging after every second cycle of treatment. Patients with suspicious physical findings or complaints were restaged early as clinically indicated. Consistent with the fact that most patients discontinued treatment for disease progression after 2 or fewer treatment cycles, no objective responses were observed. The median time to progression (TTP) was 8 weeks, but several of the NSCLC and RCC patients had disease stabilization beyond initial restaging. One of the RCC patients treated at the 0.5 mcg/kg dose level had stabilization of small volume lung disease for 2 years. Interestingly, this patient's lesions were growing prior to treatment, and he experienced regrowth of his lung metastases within 8 months of cessation of treatment, suggesting that rhIL15 antitumor effects played a role in his disease stabilization.

Pharmacokinetics and production of inflammatory cytokines

The time of maximum drug concentration (T_{max}) was found to occur 4 hours following subcutaneous administration of rhIL15 (Fig. 1A), which was noticeable beginning at the 1 mcg/kg dose level. The maximum drug concentration (C_{max}) at this time point increased proportionally with higher dose levels of rhIL15 so that the arithmetic mean value for the C_{max} (± 1 SD) was <30 (± 0) pg/mL, 87 (± 50) pg/mL, 624 (± 714) pg/mL, 1632 ($\pm 2,049$) pg/mL, and 6,459 (± 2180) pg/mL for the 0.25, 0.5, 1.0, 2.0, and 3.0 mcg/kg/day dose cohorts, respectively. By 24 hours postdose, the mean serum rhIL15 concentration had fallen more than one log to <30 , 38, 36, 70, and 113 pg/mL for the 5 dose levels. The nonlinear dose response for the C_{max} value is most consistent with a pharmacokinetic model of more complete clearance of serum rhIL15 at the lower dose levels due to greater availability of high-affinity IL15 receptors.

Changes in serum concentrations of several important inflammatory cytokines were also evaluated. There were no consistent changes in IL1 β , IL10, and IL12p70 (data not shown). Small increases in mean IL6, IFN γ (Fig. 1B and C, respectively), and TNF α (data not shown) were seen in the 3 highest dose cohorts, mirroring the pharmacokinetics of rhIL15 and peaking at 4 hours after dosing. However, peak levels were not statistically different among dose cohorts. IL6 levels were slightly elevated but significantly lower than IL6 levels seen with cytokine release syndrome from chimeric antigen receptor gene–modified T cells (41). Given the overall higher levels of IFN γ detected, it is more likely that IFN γ levels corresponded with the postinjection onset of fevers in treated patients.

Lymphocyte expansion and immune activation in lymphocyte subsets

Serial analyses of absolute lymphocyte counts (ALC) and flow cytometric assessment of lymphocyte subsets revealed significant increases in ALC and circulating NK-cell numbers respectively beginning with the initial dose level (Fig. 2A and B). The mean maximum posttreatment ALC increase during cycle 1 was 1.5, 2.4, 2.3, 3.9, and 8.2-fold, respectively, for the 5 dose levels, whereas the maximum posttreatment WBC increase was 1.1, 1.9, 1.3, 1.4, and 2.0-fold. A dramatic increase in the number of circulating NK cells produced mean 2.3, 3.3, 4.4, 10.8, and 13.5-fold increases respectively for the 5 dose levels (Fig. 2C). Increases in the number

Miller et al.

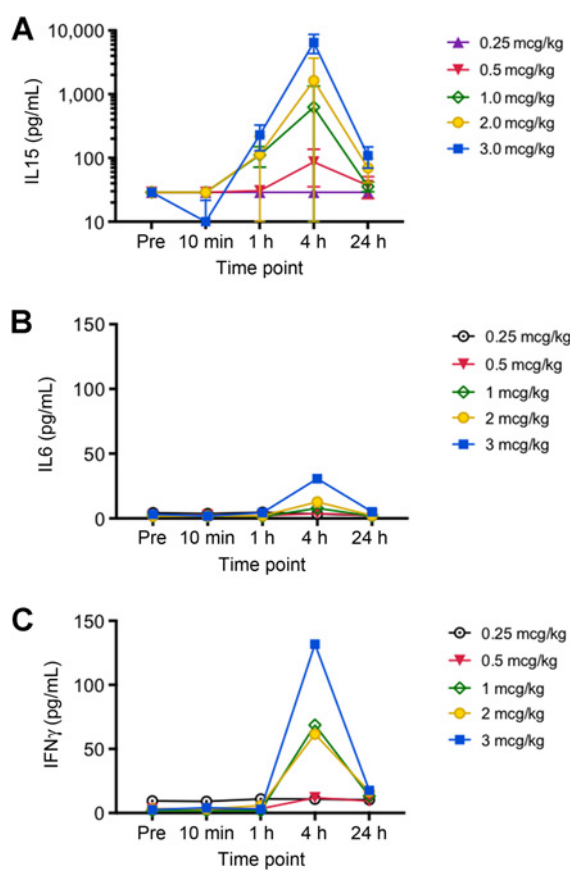


Figure 1. rhIL15 pharmacokinetics and cytokine responses. Blood samples were collected from enrolled subjects before, and 10 minutes, 1, 4, and 24 hours after the first dose of rhIL15 given subcutaneously during cycle 1. Serum was frozen until batch ELISA testing was performed for IL15 (A), IL6 (B), and IFN γ (C) levels, as described in Materials and Methods. Mean results from each dose cohort are shown with error bars (± 1 SD); the y-axis is shown in log (A) or linear scales (B and C). Error bars for B and C were omitted to facilitate viewing of the data because error bars for all dose cohorts overlapped, even at the 4-hour peak time point.

of circulating CD8⁺ effector cells were modest, with mean maximal 3.3- and 2.8-fold increases over baseline at the 2 and 3 mcg/kg dose levels, respectively. Maximal increases in NK and CD8⁺ T-cell numbers occurred during the second week of treatment during each cycle, with peak numbers consistently on day 15, three days after the last dose of rhIL15. This observation is consistent with return of NK cells into the peripheral circulation after withdrawal from activation. Maximal increases in NK-cell numbers during cycle 2 were consistently lower than in cycle 1, suggesting tachyphylaxis of the rhIL15-induced NK-cell lymphocytosis but less evident for the ALC and CD8⁺ T-cell responses. The finding of tachyphylaxis for NK cells, but not for CD8⁺ T cells, is in agreement with observations from both mouse and nonhuman primate studies (30).

A deeper analysis indicated that both CD56^{bright} and CD56^{dim} NK cells increased in number (Fig. 3A). However, the larger CD56^{dim} subset had the highest absolute numbers posttreatment, while the smaller CD56^{bright} subset demonstrated a greater fold-increase in cell numbers (Fig. 3A). This is not unexpected as

CD56^{bright} NK cells are known to proliferate at a higher rate than CD56^{dim} NK cells. NK cell cytotoxic capacity stimulated by K562 cells *in vitro*, and measured by CD107a⁺ degranulation or TNF α ⁺ production (Fig. 3C) was maximal at the end of treatment rather than 3 days after rhIL15 cessation when NK-cell numbers peaked in the peripheral circulation. Increased expression of intracellular Ki67, a specific marker of cellular proliferation, among multiple lymphocyte subsets (Fig. 3D) corroborates the NK-cell increases, but also suggests that rhIL15-stimulated increases in T-cell subsets may be underestimated in the circulation.

Assessment of anti-rhIL15 antibodies and neutralizing activity

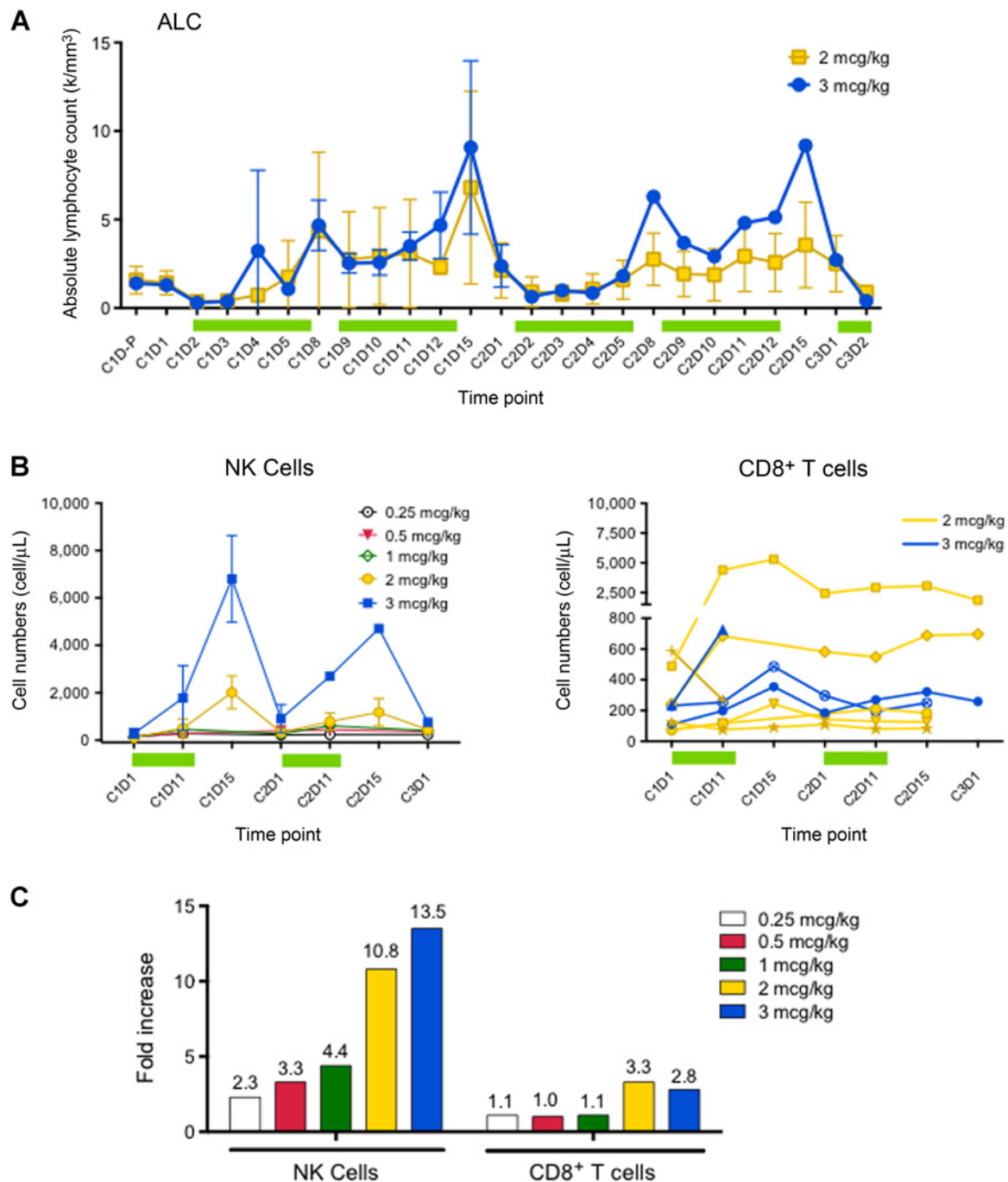
Only 3 of the 19 enrolled patients developed anti-rhIL15 antibodies (Fig. 4A); all were first detected after the third cycle of treatment. These anti-rhIL15 antibody titers continued to rise in 2 patients who continued treatment and for whom subsequent samples were available. The detection of anti-IL15 antibodies was not associated with any clinical toxicity.

The neutralizing capacity of anti-rhIL15 antibodies that developed in treated patients was evaluated using the IL15/IL2-dependent cell line NK-92 (Fig. 4B and C). The addition of anti-rhIL15 antibody-containing patient sera to cultures of NK-92 cells and exogenous rhIL15 resulted in inhibition of NK-92 cell proliferation (Fig. 4B). These results indicate that the anti-rhIL15 antibodies that developed were neutralizing for the clinical agent. However, when heterodimeric rhIL15/IL15R α was added to the NK-92 proliferation assay, patient serum exhibited only a partial functional suppression of proliferation (Fig. 4C). These results demonstrate the relative specificity of the neutralizing anti-IL15 antibodies against the single-chain *E. coli* rhIL15 used for treatment compared with the physiologic heterodimeric IL15/IL15R α that is active *in vivo*.

Discussion

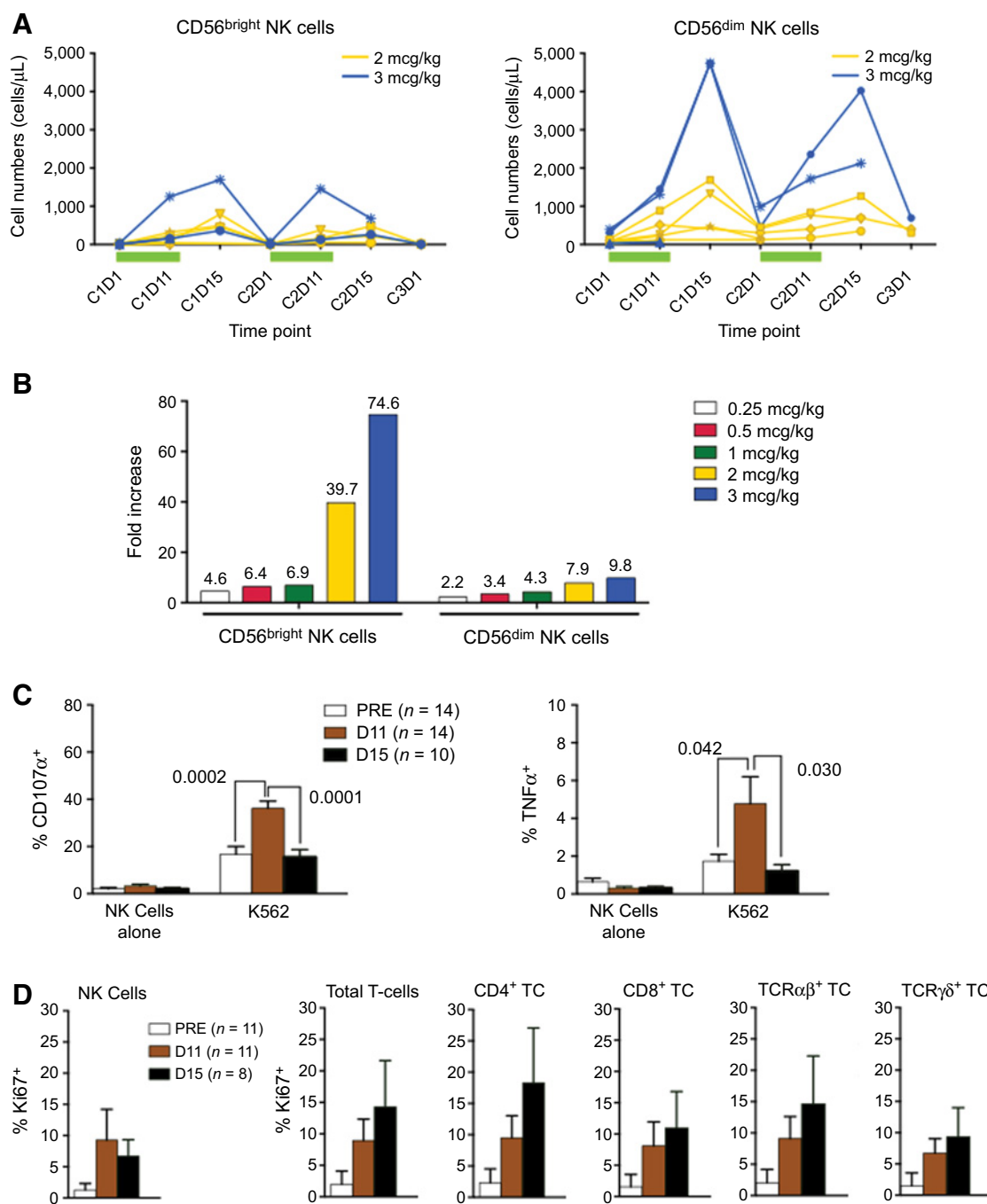
The primary goal of this phase I dose escalation trial, to identify the maximum safe and tolerable dose of SC rhIL15 that could be administered on an outpatient basis, was achieved. Subject 10 (2 mcg/kg) experienced an SAE of pancreatitis that resolved fully within a few weeks without sequelae and subject 18 (3 mcg/kg) had an SAE and dose-limiting grade 3 cardiac chest pain that also resolved quickly after discontinuation of treatment with supportive care. Apart from these two events, the spectrum of AEs was generally found to be mild and reversible. Dose-dependent AEs were most often immunomodulatory cytokine toxicities such as mild chills, fevers, fatigue, nausea/vomiting, and skin changes that could be lessened or eliminated with standard antipyretics or antiemetics. Mild and/or transient decreases in blood pressure, red blood cells, platelets, and white blood cells also seemed dose dependent, but did not result in consequential clinical adverse events, exemplifying a good composite safety profile. The primary goal of this study was to establish a safe outpatient dose for subcutaneous rhIL15, and we determined 2 mcg/kg to be the MTD.

Demonstration of a clinical effect in single-agent phase I trials is rare, and was not seen in this trial. The patients entered in this trial were generally older (median age 61 and 32% >70 years) and heavily pretreated. Seven of the patients had stable disease (SD) and continued treatment beyond initial restaging, including a RCC patient (subject 5) who remained on treatment for 2 years

**Figure 2.**

Circulating lymphocyte, NK and CD8⁺ T-cell numbers before and during rhIL15 treatment. Absolute lymphocyte counts were calculated from CBC data obtained daily from individual subjects' local labs for the 2 mcg/kg/day (yellow, $n = 6$) and 3 mcg/kg/day (blue, $n = 3$) dose cohorts, and includes a pre-cycle 1 day (CID-P) time point (A). Each line/symbol represents mean results from each dose cohort with error bars (± 1 SD). Green bars represent periods of daily rhIL15 treatment. Absolute cell frequencies (cells/mL) of CD45⁺CD3⁺CD56⁺ NK cells in fresh whole blood were measured using Trucount tubes and are shown as means (± 1 SD) grouped by dose cohort (B, left). Absolute cell frequencies (cells/mL) of CD45⁺CD3⁺CD8⁺ T cells among subjects treated with 2 or 3 mcg/kg/day of rhIL15 is shown (B, right). Each line/symbol represents results from a single individual from the 2 and 3 mcg/kg/day levels as shown in A. Mean fold increases for whole-blood NK- and CD8⁺ T-cell frequencies during cycle 1 at days 11 or 15 (whichever was available and/or maximal) compared with baseline (day 1) for all treated subjects is shown, grouped by dose cohort (C). Mean CD56⁺ NK-cell fold increases (± 1 SD) for the 0.25 ($n = 3$), 0.5 ($n = 3$), 1 ($n = 3$), 2 ($n = 6$), and 3 ($n = 3$) mcg/kg dose cohorts were 2.3 (± 1.2), 3.3 (± 2.3), 4.4 (± 3.2), 10.8 (± 8.2), and 13.5 (± 6.6), respectively. Mean CD8⁺ T-cell fold increases (± 1 SD) for the 0.25, 0.5, 1, 2, and 3 mcg/kg dose cohorts were 1.1 (± 0.2), 0.9 (± 0.2), 1.2 (± 0.2), 3.3 (± 3.8), and 2.8 (± 0.6), respectively.

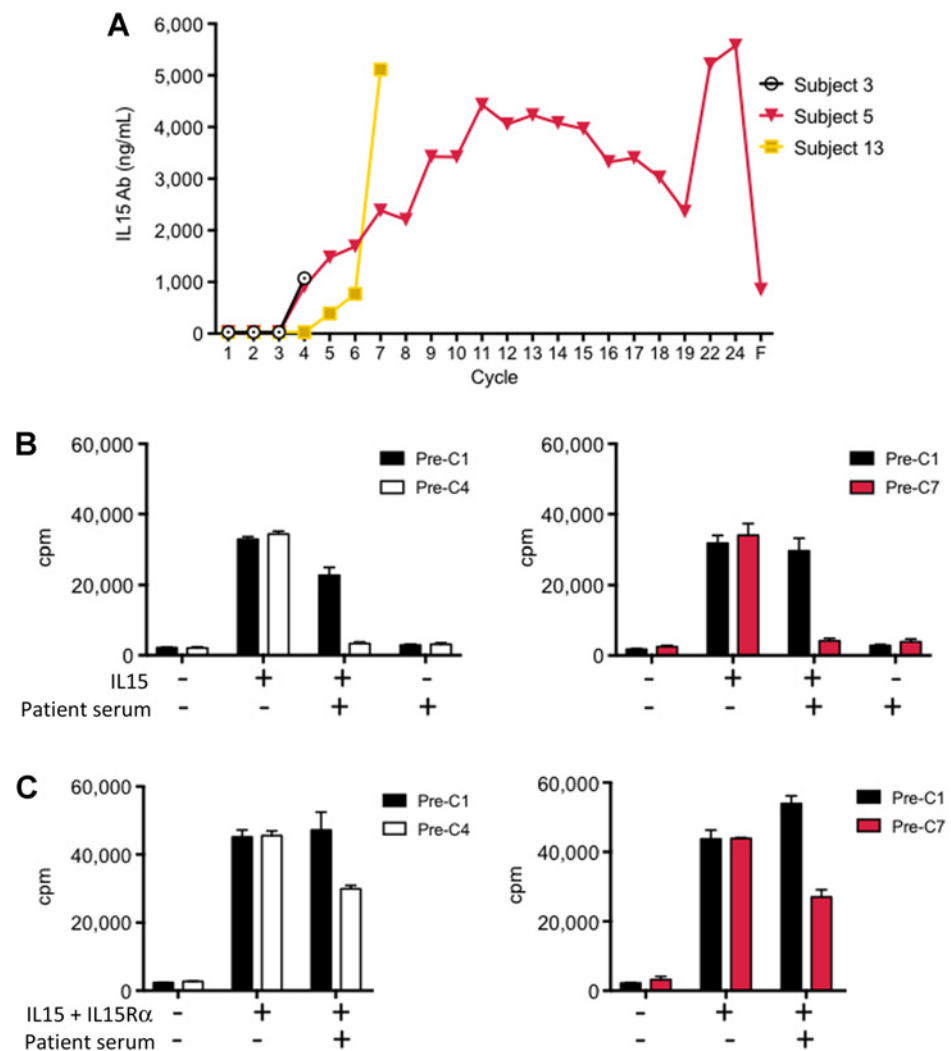
Miller et al.

**Figure 3.**

Circulating NK-cell subset expansion and NK-cell function during rhIL15 treatment. Whole-blood samples were analyzed for CD3⁻ CD56⁺ NK-cell subset frequencies of CD56^{bright} (left) and CD56^{dim} (right) NK cells using multiparametric flow cytometry as described in **A**. Individual subject data are represented by a single line/symbol, in yellow for the 2 mcg/kg/day ($n = 6$) and blue for the 3 mcg/kg/day ($n = 4$) dose cohorts (**A**). Green bars represent periods of daily rhIL15 treatment. Mean fold-increases during cycle 1 at days 11 or 15 (whichever was available and/or maximal) compared with baseline (day 1) for treated subjects, grouped by dose cohort, are indicated by each column for whole blood CD56^{bright} and CD56^{dim} NK cells (**B**). Mean CD56^{bright} NK-cell fold increases (\pm 1 SD) for the 0.25 ($n = 3$), 0.5 ($n = 3$), 1 ($n = 3$), 2 ($n = 6$), and 3 ($n = 4$) mcg/kg dose cohorts were 4.6 (\pm 1.6), 6.4 (\pm 4.1), 6.9 (\pm 2.2), 39.7 (\pm 54.4), and 74.6 (\pm 74.4), respectively. Mean CD56^{dim} NK-cell fold increases (\pm 1 SD) for the 0.25, 0.5, 1, 2, and 3 mcg/kg dose cohorts were 2.2 (\pm 1.2), 3.4 (\pm 2.5), 4.3 (\pm 3.6), 7.9 (\pm 4.7), and 9.8 (\pm 7.0), respectively. Mean values are shown above each column. Cryopreserved samples obtained before rhIL15 initiation ($n = 11$) and at day 11 ($n = 11$) and day 15 ($n = 8$) during/after treatment were assessed for evidence of active proliferation by intracellular Ki67 labeling of NK cells, T cells, and T-cell subsets as described in **C**. NK-cell degranulation (**D**, left) or intracellular TNF α (**D**, right) measured after no stimulation or stimulation with K562 for 5 hours is shown.

Figure 4.

Development of anti-rhIL15 antibodies and assessment of neutralizing capacity. All enrolled subjects were tested for the presence of anti-rhIL15 serum antibodies at baseline, at the start of each cycle, and at their final blood draw for correlative testing. Of 19 subjects, only 3 developed antibodies against rhIL15, and serum antibody levels for these 3 subjects are shown (A). For the graph x-axis in A, "F" refers to the 6-month follow-up visit after study withdrawal. Serum from two subjects, subject 3 (0.25 mcg/kg/day, white and black bars) and subject 5 (0.5 mcg/kg/day, red and black bars) were tested for their ability to inhibit the proliferation of NK92, an IL15-dependent cell line, in the presence of rhIL15 (B) or rhIL15 + IL15 receptor- α (C) in a ^3H -thymidine incorporation assay. Means of triplicate values ± 1 SD are shown.



with SD and had continued stable disease for an additional 8 months before beginning other treatment. The SC IL15 treatment produced only a modest circulating CD8⁺ T lymphocytosis, although Ki67 analyses suggested that these data may underestimate the effect of rhIL15 on T cells. More encouraging, SC rhIL15 proved to be a forceful stimulator of human NK cells, generating a 10-fold expansion of highly functional NK cells at the 2 highest doses that was equivalent to the level of NK-cell expansion in non-human primates treated with 20 mcg/kg (37). The fold-increase in NK cells was greater in the small population of CD56^{bright} NK cells relative to CD56^{dim} NK cells, with absolute numbers greatest in both subsets 3 days after the last dose of rhIL15 in cycle 1. In contrast, NK-cell function peaked shortly after the last IL15 dose and rapidly diminished several days thereafter, possibly due to cytokine withdrawal terminating a cumulative effect on activation and/or trafficking of activated cells into tissues from the peripheral blood.

Preliminary pharmacokinetic analyses indicated the time to maximum rhIL15 concentration postinjection is approximately 4 hours. Even in the two highest dose cohorts, the 24-hour serum rhIL15 concentrations had decreased more than one log from the 4-hour peak value, therefore supporting a daily treatment sched-

ule for SC rhIL15. The similar kinetics of rhIL15 C_{max} and inflammatory cytokines IL6 and IFN γ was not surprising.

For patients treated with recombinant human protein agents, the development of anti-drug antibodies (ADA) is not uncommon. Furthermore, subcutaneous administration of these drugs would potentially make them more immunogenic and thus more likely to elicit an ADA response. Although these antibodies are often clinically inconsequential with regard to efficacy or toxicity, *E. coli*-derived nonglycosylated proteins have high potential for inducing consequential ADAs because of their dissimilarity from mammalian glycoproteins. The original rhIL7 formulation which required a new mammalian cell line production method to address neutralizing ADAs that prohibited repeat dosing in patients is a cautionary tale (42). While three intermediate dose level patients treated with multiple cycles of rhIL15 in this study developed progressively increasing titers of neutralizing ADAs, these antibodies had no apparent clinical consequence. This is best exemplified by subject 5, who seemingly experienced the greatest clinical benefit from rhIL15 treatment (SD for 2 years), but also had the highest ADA levels. Although more attention to this phenomenon will still be required in future, subcutaneous rhIL15 trials with patients evaluated over multiple cycles, results

Miller et al.

from this trial suggest that ADA seen in this study are not an obstacle for the physiologic activity of IL15 when transpresented as a complex with IL15R α .

While preclinical animal model testing identifies the basic immunologic events anticipated to occur in humans, initial clinical efforts with new agents often identify new toxicities or demonstrate important dissimilarities among murine, macaque, and human physiology. The initial first-in-human clinical trial with rhIL15 administered as an IVB was unexpectedly and severely limited in dose escalation, produced diminutive immune activation, and thereby demonstrated little potential for use in combination with other agents. In the current study, new or problematic toxicities were not identified and subcutaneous dosing allowed 6-fold more drug administration compared with IVB. In fact, adverse effects associated with daily SC rhIL15 injection were mild, well-tolerated, and manageable on an outpatient basis, making rhIL15 amenable to future combination with other therapies. IL15 may also be broadly applied to immunotherapy for other diseases, although we need to be cautious about hematologic malignancies that might actually be stimulated by IL15. In addition to defining the basic safety goals, a deeper understanding of treatment-related functional changes in responsive effector cell subsets was a critical objective for this research. In summary, using an outpatient regimen of subcutaneous IL15, these analyses revealed robust effects on immune effector NK cells primarily, with lesser effects on CD8⁺ T cells, which will inform the design of future combination rhIL15 treatment regimens including NK- (15, 16, 43) or T-cell infusions (4–7), checkpoint inhibitors (1–3) and multiple FDA-approved cancer-targeting antibodies.

Disclosure of Potential Conflicts of Interest

D. G. McNeel holds ownership interest (including patents) in and is a consultant/advisory board member for Madison Vaccines Inc. No potential conflicts of interest were disclosed by the other authors.

References

- Borghaei H, Paz-Ares L, Horn L, Spigel DR, Steins M, Ready NE, et al. Nivolumab versus docetaxel in advanced nonsquamous non-small-cell lung cancer. *N Engl J Med* 2015;373:1627–39.
- Brahmer JR, Tykodi SS, Chow LQ, Hwu WJ, Topalian SL, Hwu P, et al. Safety and activity of anti-PD-L1 antibody in patients with advanced cancer. *N Engl J Med* 2012;366:2455–65.
- Topalian SL, Hodi FS, Brahmer JR, Gettinger SN, Smith DC, McDermott DF, et al. Safety, activity, and immune correlates of anti-PD-1 antibody in cancer. *N Engl J Med* 2012;366:2443–54.
- Weber J, Atkins M, Hwu P, Radvanyi L, Sznol M, Yee C, et al. White paper on adoptive cell therapy for cancer with tumor-infiltrating lymphocytes: a report of the CTIEP subcommittee on adoptive cell therapy. *Clin Cancer Res* 2011;17:1664–73.
- Rosenberg SA, Yang JC, Sherry RM, Kammula US, Hughes MS, Phan GQ, et al. Durable complete responses in heavily pretreated patients with metastatic melanoma using T-cell transfer immunotherapy. *Clin Cancer Res* 2011;17:4550–7.
- Lee DW, Kochenderfer JN, Stetler-Stevenson M, Cui YK, Delbrook C, Feldman SA, et al. T cells expressing CD19 chimeric antigen receptors for acute lymphoblastic leukaemia in children and young adults: a phase 1 dose-escalation trial. *Lancet* 2015;385:517–28.
- Maude SL, Frey N, Shaw PA, Aplenc R, Barrett DM, Bunin NJ, et al. Chimeric antigen receptor T cells for sustained remissions in leukemia. *N Engl J Med* 2014;371:1507–17.
- Dudley JC, Lin MT, Le DT, Eshleman JR. Microsatellite instability as a biomarker for PD-1 blockade. *Clin Cancer Res* 2016;22:813–20.
- Gatalica Z, Snyder C, Maney T, Ghazalpour A, Holterman DA, Xiao N, et al. Programmed cell death 1 (PD-1) and its ligand (PD-L1) in common cancers and their correlation with molecular cancer type. *Cancer Epidemiol Biomarkers Prev* 2014;23:2965–70.
- Le DT, Uram JN, Wang H, Bartlett BR, Kemberling H, Eyring AD, et al. PD-1 blockade in tumors with mismatch-repair deficiency. *New Engl J Med* 2015;372:2509–20.
- Maude SL, Teachey DT, Porter DL, Grupp SA. CD19-targeted chimeric antigen receptor T-cell therapy for acute lymphoblastic leukemia. *Blood* 2015;125:4017–23.
- Ahmed N, Brawley VS, Hegde M, Robertson C, Ghazi A, Gerken C, et al. Human epidermal growth factor receptor 2 (HER2) -specific chimeric antigen receptor-modified T cells for the immunotherapy of HER2-positive sarcoma. *J Clin Oncol* 2015;33:1688–96.
- Robbins PF, Kassim SH, Tran TL, Crystal JS, Morgan RA, Feldman SA, et al. A pilot trial using lymphocytes genetically engineered with an NY-ESO-1-reactive T-cell receptor: long-term follow-up and correlates with response. *Clin Cancer Res* 2015;21:1019–27.
- Tran E, Turcotte S, Gros A, Robbins PF, Lu YC, Dudley ME, et al. Cancer immunotherapy based on mutation-specific CD4⁺ T cells in a patient with epithelial cancer. *Science* 2014;344:641–5.
- Miller JS, Soignier Y, Panoskaltis-Mortari A, McNamee SA, Yun GH, Fautsch SK, et al. Successful adoptive transfer and in vivo expansion of human haploidentical NK cells in patients with cancer. *Blood* 2005;105:3051–7.
- Bachanova V, Cooley S, Defor TE, Verneris MR, Zhang B, McKenna DH, et al. Clearance of acute myeloid leukemia by haploidentical natural killer

Authors' Contributions

Conception and design: J.S. Miller, H.E.K. Kohrt, P.M. Sondel, H.A. Wakelee, M.A. Cheever, H. Streicher, T.A. Waldmann, K.C. Conlon

Development of methodology: J.S. Miller, C. Morishima, J.A. Thompson, J.C. Kaiser, T.A. Waldmann

Acquisition of data (provided animals, acquired and managed patients, provided facilities, etc.): J.S. Miller, C. Morishima, D.G. McNeel, M.R. Patel, J.A. Thompson, H.A. Wakelee, M.L. Disis, M.A. Cheever, T.A. Waldmann, K.C. Conlon

Analysis and interpretation of data (e.g., statistical analysis, biostatistics, computational analysis): J.S. Miller, C. Morishima, J.A. Thompson, P.M. Sondel, M.L. Disis, M.A. Cheever, T.A. Waldmann, K.C. Conlon

Writing, review, and/or revision of the manuscript: J.S. Miller, C. Morishima, D.G. McNeel, H.E.K. Kohrt, J.A. Thompson, P.M. Sondel, H.A. Wakelee, M.L. Disis, J.C. Kaiser, M.A. Cheever, T.A. Waldmann, K.C. Conlon

Administrative, technical, or material support (i.e., reporting or organizing data, constructing databases): C. Morishima, J.C. Kaiser, M.A. Cheever, S.P. Creekmore, T.A. Waldmann

Study supervision: J.S. Miller, J.C. Kaiser, M.A. Cheever, H. Streicher, T.A. Waldmann, K.C. Conlon

Acknowledgments

Cancer Immunotherapy Trials Network (CITN) was supported by NIH 1U01 CA154967-01 (ClinicalTrials.gov NCT01727076). This study was also partially supported by the Intramural Research Program of the National Cancer Institute and P01 CA111412 and NCI R35 CA197292 (to J.S. Miller). The authors would like to acknowledge the contributions of the following individuals to this work: Minjun Apodaca, ASCP, and other members of the CITN Central Laboratory for their technical contributions, Stephen C. De Rosa MD and Tiffany Hensley-McBain of the HIV Vaccine Trials Network for their help in establishing the flow cytometric methods, the Fred Hutchinson Cancer Research Center Flow Cytometry Facility for their support in conducting testing, Valarie McCullar from the Miller laboratory at the University of Minnesota for functional assay testing, and Angela Riggins for her help in preparation of the manuscript figures.

The costs of publication of this article were defrayed in part by the payment of page charges. This article must therefore be hereby marked *advertisement* in accordance with 18 U.S.C. Section 1734 solely to indicate this fact.

Received August 22, 2017; revised October 22, 2017; accepted November 21, 2017; published OnlineFirst December 4, 2017.

- cells is improved using IL-2 diphtheria toxin fusion protein. *Blood* 2014;123:3855–63.
17. Maccalli C, Parmiani G, Ferrone S. Immunomodulating and immunoresistance properties of cancer-initiating cells: implications for the clinical success of immunotherapy. *Immunol Invest* 2017;46:221–38.
 18. Wang M, Busutil RA, Pattison S, Neeson PJ, Boussioutas A. Immunological battlefield in gastric cancer and role of immunotherapies. *World J Gastroenterol* 2016;22:6373–84.
 19. Wang K, Vella AT. Regulatory T cells and cancer: a two-sided story. *Immunol Invest* 2016;45:797–812.
 20. Tao J-H, Cheng M, Tang J-P, Liu Q, Pan F, Li X-P, et al. Foxp3, regulatory T cell, and autoimmune diseases. *Inflammation* 2017;40:328–39.
 21. Gabrilovich DI, Nagaraj S. Myeloid-derived suppressor cells as regulators of the immune system. *Nat Rev Immunol* 2009;9:162–74.
 22. Soliman H, Mediavilla-Varela M, Antonia S. Indoleamine 2,3-dioxygenase: is it an immune suppressor? *Cancer J* 2010;16:354–9.
 23. Waldmann TA, Lugli E, Roederer M, Perera LP, Smedley JV, Macallister RP, et al. Safety (toxicity), pharmacokinetics, immunogenicity, and impact on elements of the normal immune system of recombinant human IL-15 in rhesus macaques. *Blood* 2011;117:4787–95.
 24. Wen B, Zhang M, Dilillo D, Ravetch JV, Waldmann TA. Abstract 1332: Interleukin-15 enhances rituximab-dependent cytotoxicity ex vivo and in vivo against a mouse lymphoma expressing human CD20. *Cancer Res* 2015;75:1332–1332.
 25. Waldmann TA. The shared and contrasting roles of IL2 and IL15 in the life and death of normal and neoplastic lymphocytes: implications for cancer therapy. *Cancer Immunol Res* 2015;3:219–27.
 26. Waldmann TA, Tagaya Y. The multifaceted regulation of interleukin-15 expression and the role of this cytokine in NK cell differentiation and host response to intracellular pathogens. *Annu Rev Immunol* 1999;17:19–49.
 27. Waldmann TA. The biology of interleukin-2 and interleukin-15: implications for cancer therapy and vaccine design. *Nat Rev Immunol* 2006;6:595–601.
 28. Fehniger TA, Caligiuri MA. Interleukin 15: biology and relevance to human disease. *Blood* 2001;97:14–32.
 29. Marks-Konczalik J, Dubois S, Losi JM, Sabzevari H, Yamada N, Feigenbaum L, et al. IL-2-induced activation-induced cell death is inhibited in IL-15 transgenic mice. *Proc Natl Acad Sci U S A* 2000;97:11445–50.
 30. Sneller MC, Kopp WC, Engelke KJ, Yovandich JL, Creekmore SP, Waldmann TA, et al. IL-15 administered by continuous infusion to rhesus macaques induces massive expansion of CD8+ T effector memory population in peripheral blood. *Blood* 2011;118:6845–8.
 31. Kobayashi H, Dubois S, Sato N, Sabzevari H, Sakai Y, Waldmann TA, et al. Role of trans-cellular IL-15 presentation in the activation of NK cell-mediated killing, which leads to enhanced tumor immunosurveillance. *Blood* 2005;105:721–7.
 32. Zhang M, Yao Z, Dubois S, Ju W, Müller JR, Waldmann TA. Interleukin-15 combined with an anti-CD40 antibody provides enhanced therapeutic efficacy for murine models of colon cancer. *Proc Natl Acad Sci U S A* 2009;106:7513–8.
 33. Klebanoff CA, Finkelstein SE, Surman DR, Lichtman MK, Gattinoni L, Theoret MR, et al. IL-15 enhances the in vivo antitumor activity of tumor-reactive CD8+ T cells. *Proc Natl Acad Sci U S A* 2004;101:1969–74.
 34. Kudo-Saito C, Wansley EK, Gruys ME, Wiltrout R, Schlom J, Hodge JW. Combination therapy of an orthotopic renal cell carcinoma model using intratumoral vector-mediated costimulation and systemic interleukin-2. *Clin Cancer Res* 2007;13:1936–46.
 35. Fyfe G, Fisher RI, Rosenberg SA, Sznol M, Parkinson DR, Louie AC. Results of treatment of 255 patients with metastatic renal cell carcinoma who received high-dose recombinant interleukin-2 therapy. *J Clin Oncol* 1995;13:688–96.
 36. Rosenberg SA, Lotze MT, Yang JC, Topalian SL, Chang AE, Schwartzentruber DJ, et al. Prospective randomized trial of high-dose interleukin-2 alone or in conjunction with lymphokine-activated killer cells for the treatment of patients with advanced cancer. *J Natl Cancer Inst* 1993;85:622–32.
 37. Conlon KC, Lugli E, Welles HC, Rosenberg SA, Fojo AT, Morris JC, et al. Redistribution, hyperproliferation, activation of natural killer cells and CD8 T cells, and cytokine production during first-in-human clinical trial of recombinant human interleukin-15 in patients with cancer. *J Clin Oncol* 2015;33:74–82.
 38. Hensley TR, Easter AB, Gerds SE, De Rosa SC, Heit A, McElrath MJ, et al. Enumeration of major peripheral blood leukocyte populations for multicenter clinical trials using a whole blood phenotyping assay. *J Vis Exp* 2012:e4302.
 39. Meager A, Wadhwa M. Detection of anti-cytokine antibodies and their clinical relevance. *Expert Rev Clin Immunol* 2014;10:1029–47.
 40. Iasonos A, Wilton AS, Riedel ER, Seshan VE, Spriggs DR. A comprehensive comparison of the continual reassessment method to the standard 3 + 3 dose escalation scheme in Phase I dose-finding studies. *Clin Trials* 2008;5:465–77.
 41. Lee DW, Gardner R, Porter DL, Louis CU, Ahmed N, Jensen M, et al. Current concepts in the diagnosis and management of cytokine release syndrome. *Blood* 2014;124:188–95.
 42. Sportès C, Babb RR, Krumlauf MC, Hakim FT, Steinberg SM, Chow CK, et al. Phase I study of recombinant human interleukin-7 administration in subjects with refractory malignancy. *Clin Cancer Res* 2010;16:727–35.
 43. Pérez-Martínez A, Fernández L, Valentín J, Martínez-Romera I, Corral MD, Ramírez M, et al. A phase I/II trial of interleukin-15-stimulated natural killer cell infusion after haplo-identical stem cell transplantation for pediatric refractory solid tumors. *Cytotherapy* 2015;17:1594–603.

Clinical Cancer Research

A First-in-Human Phase I Study of Subcutaneous Outpatient Recombinant Human IL15 (rhIL15) in Adults with Advanced Solid Tumors

Jeffrey S. Miller, Chihiro Morishima, Douglas G. McNeel, et al.

Clin Cancer Res 2018;24:1525-1535. Published OnlineFirst December 4, 2017.

Updated version Access the most recent version of this article at:
doi:[10.1158/1078-0432.CCR-17-2451](https://doi.org/10.1158/1078-0432.CCR-17-2451)

Cited articles This article cites 42 articles, 24 of which you can access for free at:
<http://clincancerres.aacrjournals.org/content/24/7/1525.full#ref-list-1>

Citing articles This article has been cited by 15 HighWire-hosted articles. Access the articles at:
<http://clincancerres.aacrjournals.org/content/24/7/1525.full#related-urls>

E-mail alerts [Sign up to receive free email-alerts](#) related to this article or journal.

Reprints and Subscriptions To order reprints of this article or to subscribe to the journal, contact the AACR Publications Department at pubs@aacr.org.

Permissions To request permission to re-use all or part of this article, use this link
<http://clincancerres.aacrjournals.org/content/24/7/1525>.
Click on "Request Permissions" which will take you to the Copyright Clearance Center's (CCC) Rightslink site.